Polymer 51 (2010) 5151–5164

Contents lists available at ScienceDirect

Polymer

journal homepage: www.elsevier.com/locate/polymer

Polymer electrolytes based on a ternary miscible blend of poly(ethylene oxide), poly(bisphenol A-*co*-epichlorohydrin) and poly(vinyl ethyl ether)

Ana Maria Rocco [a,*], Alexander de Assis Carias [a], Robson Pacheco Pereira [b]

[a] Grupo de Materiais Condutores e Energia, Escola de Química, Universidade Federal do Rio de Janeiro, Av. Horácio Macedo, 2030, Rio de Janeiro 21941-909, Brazil
[b] Instituto de Ciências Exatas (ICEx), Pólo Universitário de Volta Redonda, Universidade Federal Fluminense, Volta Redonda, Rio de Janeiro, Brazil

ARTICLE INFO

Article history:
Received 2 June 2010
Received in revised form
12 August 2010
Accepted 21 August 2010
Available online 27 August 2010

Keywords:
Miscibility
Lithium ion conduction
Interactions

ABSTRACT

Ternary blends of poly(ethylene oxide) (PEO), poly(bisphenol A-*co*-epichlorohydrin) (PBE) and poly(vinyl ethyl ether) (PVEE) were obtained as films and characterized by differential scanning calorimetry (DSC) and vibrational spectroscopy (FTIR). From the DSC results, phase diagrams for the ternary blends were determined, where the variation of the viscoelastic phase extent as a function of the polymers composition was determined. The DSC results also indicated miscibility of the system, exhibiting only one glass transition temperature (T_g) and decrease in the crystallinity of the system, as well as decrease in the crystallinity of PEO present in the blends. Vibrational spectroscopy (FTIR) provided information on the intermolecular interactions between the pairs PBE/PEO and PBE/PVEE, *via* hydrogen bond interaction. From the FTIR analyses, molecular model systems of equilibrium among the interacting structures were proposed as a molecular basis for the miscibility of the system.

Polymer electrolytes based on the ternary blend containing 60/25/15 (PEO/PBE/PVEE) mass percent and lithium perchlorate ($LiClO_4$) were obtained and characterized by DSC, FTIR, optical microscopy and electrochemical impedance spectroscopy (EIS). Solid electrolytes containing up to 10 wt% $LiClO_4$ exhibited a single-phase behavior, evidenced by the DSC results. For these electrolytes, FTIR spectra indicated the formation of polymer–ion complexes, in which the cation (Li^+) acts favoring the polymer–polymer miscibility. Electrolytes containing $LiClO_4$ higher than 10 wt% exhibit a multiple phase behavior, in which a PEO-rich, salt-containing phase is present in equilibrium with PBE or PVEE-rich phases. Maximum ionic conductivity at room temperature, for the electrolyte containing 20 wt% $LiClO_4$, reached $4.23 \times 10^{-3}\ \Omega^{-1}\ cm^{-1}$, while all samples exhibited conductivity of approximately $10^{-1}\ \Omega^{-1}\ cm^{-1}$ at 80 °C.

1. Introduction

The development, optimization and production of a wide range of devices, from portable phones and notebooks to electrical vehicles and residential power stations, depends mainly on the development of more efficient materials for application as electrodes and electrolytes, which are the key components in lithium batteries [1]. More recently, the commercialization of electrical vehicles, especially the ones powered by lithium-ion batteries, has promoted even more the interest in the development of materials, power devices and auxiliary systems for such technology. As important as the scientific and technological aspects, there is an urgency to reduce the fossil fuel consumption which, in the last two centuries, has markedly influenced on the global climate change [2].

PEO-salt electrolytes present highly crystalline structures [3], which induce the decrease of ionic mobility [4], since the conduction takes place primarily in the non-crystalline regions. However, some structural order in these non-crystalline regions is advantageous for increasing ionic conductivity, as pointed out by Bruce and co-workers [5]. PEO possesses a relatively simple structure and is capable of packing into crystals, serving as a model polymer for a wide variety of studies, including theoretical calculations [6,7], polymer blends [8–10], solid electrolytes [11], structural and nanostructural characterization [12], among others. Since PEO exhibits high crystallinity and, consequently, restricted segmental motion, blending is considered an alternative to decrease the overall crystallinity, keeping part of the structural order of the crystalline phase in the solid [13], also lowering melting point as well as the crystallinity degree and optimizing the nanostructure of such materials, which enhances the conductivity of the electrolyte [14]. The incorporation of a low-molecular weight polymer, which can induce a plasticizer effect, can favor the chain mobility and,

* Corresponding author. Fax: +55 21 2562 7567.
E-mail address: amrocco@eq.ufrj.br (A.M. Rocco).

0032-3861/$ – see front matter © 2010 Elsevier Ltd. All rights reserved.
doi:10.1016/j.polymer.2010.08.050

consequently, the applicability of the blend as a host for ion-conductive systems. Binary blends often exhibit multiphase behavior [15], which may compromise the properties of the system and limit its applicability and, in this regard, the addition of a third component to a binary blend can be considered an alternative to obtain miscible polymer matrices with optimized properties [16,17]. The fine tuning of the miscibility between polymers can be obtained, for instance, with the addition of a component which is able to interact specifically with both chains, *via* hydrogen bonding or other interactions.

Poly(bisphenol A-*co*-epichlorohydrin) (phenoxy or PBE) is a widely studied polymer and is considered as a model of epoxy resin [18,19]. Robeson and co-workers [20], studying blends of PBE with water-soluble polymers showed that PBE could act as a proton donor, due to the presence of a hydroxyl group in the polymer chain. Blends of PEO of high molecular weight with PBE of high epoxy equivalent were studied spectroscopically, thermally and morphologically earlier [21] and exhibited miscibility over the entire range of compositions. Thermal and morphological properties of this system were evaluated and a model for interactions between the PEO and PBE was established by vibrational spectroscopy (FTIR). Analysis of the spectroscopic fractions from FTIR spectra provided quantification of the specific interactions *via* hydrogen bonding between the polymers and its dependence on the blend composition.

The dielectric relaxation behavior of poly(vinyl ethyl ether) (PVEE) binary blends with poly(vinylphenol) (PVPh) [22], studied by Painter and co-workers, indicated that blend compositions with sufficiently large hydrogen bond fractions exhibit a single relaxation process. Similar systems without specific interactions present more than one relaxation process, evidencing the key role of hydrogen bonding to the miscibility of the PVEE-based systems.

Ternary blends such as PBE/PMMA/PEO [23], PVPh/poly(vinyl acetate)/PEO [24], and poly(styrene-*co*-acrylic acid)/PMMA/PEO [25] have been studied and presented phase separation caused by the difference in the interaction energy of the binary systems. As pointed out by Lin and co-workers [26], the differences between inter- and intra-association equilibrium constants (the "ΔK" effect) in PVPh-*b*-PMMA/PEO blend can lead to phase diagrams containing a closed-loop phase separated region, whereas the system PVPh-*r*-PMMA/PEO is completely miscible.

So far, a small number of ternary polymer blends have been used as host matrices in solid electrolytes, mostly due to miscibility issues, since these materials operate in a temperature range in which phase segregation may occur. In these multiphase systems, the lithium salt may be confined in one phase or distributed unevenly through the solid, leading to conductivity fluctuations which prevent the correct operation of the device in which the solid electrolyte is assembled. Studying and controlling the miscibility of such complex systems is a key issue in the application of ternary polymer blends as host for solid electrolytes.

In a previous work [27], a solid electrolyte based on a binary PEO/PBE blend was obtained, with miscibility independent of the salt ($LiClO_4$) concentration. However, there existed an optimum salt concentration where conductivity of the system reached a maximum of $10^{-5}\ \Omega^{-1}\ cm^{-1}$, probably due to the high T_g of PBE (which influences on the T_g of the solid electrolyte) and insufficient number of basic oxygen sites for Li^+ coordination. In the present work, the addition of PVEE to the PEO/PBE blend aims the decrease of T_g of the polymer matrix and an increase in the number of basic oxygen sites, in order to obtain an optimized matrix for solid electrolyte applications. The present work focuses on the properties of ternary PEO/PBE/PVEE blends, where low-molecular weight PVEE is added to a PEO/PBE binary blend.

2. Experimental

2.1. Materials

PEO ($M_w = 4 \times 10^6$ g/mol), PVEE ($M_w = 3800$ g/mol), PBE (800–950 g equiv^{-1}) and $LiClO_4$ were supplied by Aldrich Chem. Co., acetone (PA), supplied by Merck, was distilled and stored under molecular sieves. All the chemicals were utilized after drying under vacuum at 80 °C.

2.2. Samples preparation

2.2.1. Blends

Solutions of polymers in acetone were stirred for 24 h. Films of the binary PEO/PVEE, PBE/PVEE and the ternary PEO/PBE/PVEE blends were prepared by casting from these solutions onto glass plates and dried until constant weight in a desiccator under vacuum. In this study, the blends are designated by the weight percentage of their components: PEO, PBE and PVEE. As an example, the sample 70/20/10 corresponds to a ternary blend containing 70 wt% PEO, 20 wt% PBE and 10 wt% PVEE.

2.2.2. Electrolytes

Solutions of polymers and salt in acetone were stirred for 24 h at 35 °C. Electrolyte membranes were prepared by casting from these solutions onto glass plates and dried until constant weight in a desiccator under vacuum. In the present work, the PEO/PBE/PVEE mass (percent) ratio was kept constant in 60/25/15 and the salt concentration was varied from 5 to 30 wt% of the total mass. All the membranes were stored in a dry box in order to avoid humidity and all the electrochemical determinations were also performed in a dry box. Macroscopic photographs of membranes containing 10, 20 and 30 wt% $LiClO_4$ are represented in the Supplementary material, Fig. S1.

2.3. Differential scanning calorimmetry (DSC)

To evaluate the miscibility and thermal behavior of the samples, DSC measurements were performed on a General V4.1C DuPont 2100 apparatus. Samples were first heated from 25 to 150 °C at a heating rate of 10 °C min^{-1} (run I). After a 5 min isotherm, samples were cooled to −100 °C at 10 °C min^{-1} (run II) and then heated at 10 °C min^{-1} to 100 °C (run III). The melting temperatures (T_m) and apparent melting enthalpy (ΔH_m) were determined from the maximum and the area of the endothermic peaks, respectively, scaled by the mass of the samples, in the DSC curves on the run III. Glass transition temperatures (T_g) and glass transition widths (ΔT_g) were determined as described earlier [8]. The crystallinity degree of the sample (X_c for either blends or electrolytes) and of the PEO present on each sample ($X_{c,PEO}$) was calculated from Equations (1) and (2), respectively:

$$X_c = \frac{\Delta H_m}{\Delta H^o_{PEO}} \tag{1}$$

$$X_{c,PEO} = \frac{\Delta H_m}{f \cdot \Delta H^o_{PEO}} = \frac{X_c}{f} \tag{2}$$

Where f is the mass fraction of PEO present in the electrolyte (the only crystallizable polymer in the system), and ΔH^o_{PEO} is the heat of melting per gram of 100% crystalline PEO, 188 J g^{-1} [28].

2.4. Vibrational spectroscopy (FTIR)

For the vibrational spectra, samples were prepared by casting directly onto KBr pellets and films dried under vacuum. FTIR spectra were obtained on a Nicolet 760 FTIR spectrometer at room temperature, employing 128 scans with a resolution of 1 cm^{-1} and optimized gain for all samples. The humidity control was done by obtaining FTIR spectra of PEO samples prepared concomitantly and treated in the same manner as the samples of the blends.

2.5. Quantitative determinations from FTIR spectra

The perchlorate anion exhibits different infrared spectra when associated in ionic pairs as compared to the dissociated state, allowing one to separate different contributions from "free" (dissociated) and "bound" (ionic pairs or larger clusters) forms according to the mathematical treatment employed to the $\nu(ClO_4^-)$ band by Wieckzoreck and co-workers [29]. Assuming that only these two forms (free and bound) are distinguishable in IR spectra, a decomposition treatment was employed, using Gaussians as primitive functions. The total areas were then normalized and the ratio of free and associated forms was taken from the relative areas associated with each form. The hydroxyl stretching region varies markedly with hydrogen bonding, also allowing to separate different contributions from "free" (non-hydrogen bonded) and "bound" (hydrogen bonded) hydroxyl forms. Assuming these forms as the only distinguishable in the vibrational spectra, a similar decomposition treatment was employed for the ν(OH) band.

2.6. Electrochemical impedance spectroscopy (EIS)

Stainless steel electrodes were used for electrochemical impedance measurements, which were performed under dry atmosphere utilizing an EcoChemie Autolab PGSTAT30/FRA potentiostat. The range of analyzed frequencies was 10^6 to 10^{-2} Hz. Each sample was allowed to equilibrate for 1 h at a certain temperature before measurement, between 25 and 90 °C.

2.7. Cyclic voltammetry (CV)

Electrochemical stability was evaluated by cyclic voltammetry from −0.5 to 5.5 V *vs* Li with a scan rate of 1 mV s^{-1} and at a temperature of 60 °C under dry atmosphere. In order to obtain the cyclic voltamograms, the membranes were sandwiched between a stainless steel electrode and Li sheet.

3. Results and discussion

3.1. Polymer blends

3.1.1. Thermal analysis

The DSC curves (Supplementary material, Fig. S2) for binary PBE/PVEE blends do not exhibit crystallinity, as expected, since both PBE and PVEE are non-crystalline polymers. A clear and well defined single T_g for each binary PBE/PVEE blend was observed and presented a progressive decrease from the T_g of PBE (33 °C) with the PVEE concentration, which are indicatives of miscibility between PBE and PVEE. The T_g dependence on the blend composition is almost linear for high PBE concentrations, which can be associated with the nearly ideal behavior of dilute systems [30]. As noted for other PBE/polyether blends (*e.g.* with PEO), the observed T_g behavior is a consequence of the intermolecular interactions between the components. Additionally, since the low-molecular weight (viscous liquid) PVEE sample used in the present work has a T_g value of −49 °C, a nearly linear compositional dependence can be expected, especially at high concentrations.

Each of the ternary PEO/PBE/PVEE blends studied in this work present one endothermic peak (Supplementary material, Fig. S3), which is associated to the melting of the PEO crystalline phase. The apparent melting enthalpy and temperature for each sample were determined from the area and the maximum of these peaks, respectively. A slight decrease in the area of the melting peak is observed with the increase of both PBE and PVEE, which is associated with the decrease of the melting enthalpy and, consequently, the crystallinity of the system. The melting temperature of the blend also presents variations depending on the non-crystalline polymer added and the concentrations on the blend. Melting and crystallization of pure PEO samples were already described by different authors, including the paper of Pielichowski and co-workers [31], in which the step-scan alternating DSC (SSA-DSC) technique was employed to determine the reversing and non-reversing components of the heat flow. In the present work, the presence of PBE and also PVEE induces changes on the blend crystallization which can be monitored by DSC (linear scan) and are closely related to the PBE interactions with both PEO and PVEE.

In Table 1, heat capacity change during the glass transition (ΔC_p), glass transition temperature (T_g), glass transition width (ΔT_g), melting temperature (T_m), melting enthalpy ($\Delta H_{m,blend}$), and crystallinity degree ($X_{c,blend}$, $X_{c,PEO}$) for all samples are shown. The degree of crystallinity of the blend decreases from 72% (pure PEO) to 41% (blend 60/35/5), which can be a result of the miscibility among the components or a dilution effect as the PEO concentration decreases in the blend. Additionally, the degree of crystallinity of PEO present in the blend ($X_{c,blend}$ corrected by the amount of PEO in the blend) decreases to 53% for the blend 60/20/20. This indicates that the decrease in the blend global crystallinity is not only related to a dilution effect, as the crystalline structure of PEO is also affected by the presence of PBE and PVEE. Crystallization and melting of PEO blocks have also been studied by techniques such as small [32] and wide [33] angle X-ray scattering (SAXS/WAXS) and DSC. These studies show the influence of confinement on the crystallization of PEO blocks. In the present work, the decrease in PEO crystallinity is due to structural changes induced by the

Table 1
Thermal properties of PBE/PVEE, PEO/PVEE, PEO/PBE/PVEE blends and pure polymers.

Blend (PEO/PBE/PVEE)	ΔC_p ($\times 10^{-2}$ J/g °C)	ΔT_g[a] (°C)	T_g[a] (°C)	T_g (calc) (°C)	T_m[a] (°C)	$\Delta H_{m,blend}$ (J/g)	$X_{c,blend}$ (%)	$X_{c,PEO}$ (%)
100/0/0	2.4	15.0	−45	−45	72	136.0	72	72
0/100/0	9.0	24.0	33	33	–	–	–	
0/0/100	7.0	16.5	−49	−49	–	–	–	
0/85/15	9.0	23.8	8	11	–	–	–	–
0/90/10	10.0	23.6	23	18	–	–	–	–
0/95/5	11.0	29.2	15	25	–	–	–	–
95/0/5	2.6	7.1	−45	−45	73	134.8	72	76
90/0/10	2.9	4.9	−46	−45	69	132.4	70	78
80/0/20	3.1	5.8	−46	−46	67	113.7	61	76
70/0/30	3.5	9.3	−45	−46	63	110.5	59	84
60/0/40	4.8	12.7	−42	−47	61	93.1	49	82
90/5/5	2.1	17.0	−44	−41	72	130.0	69	76
80/10/10	1.0	11.0	−44	−38	62	121.0	64	80
70/15/15	1.5	11.0	−44	−34	67	72.0	38	54
70/20/10	1.1	9.7	−42	−30	66	79.8	42	60
70/25/5	1.3	10.2	−43	−26	65	74.6	40	57
60/20/20	2.0	10.0	−43	−30	65	61.0	32	53
60/25/15	1.3	8.6	−43	−26	65	61.5	33	55
60/30/10	0.5	9.2	−42	−22	66	68.7	36	60
60/35/5	1.0	8.5	−43	−23	66	77.6	41	68

[a] Temperature precision of ±1 °C.

presence of two non-crystalline polymers and the intermolecular interactions among the blend components. Ethylene oxide block copolymers with butadiene (PEO-*b*-PB) and PEO-*b*-PB/PB blends presented confined crystallization (with formation of cylindrical and spherical vesicles) without changing the crystallization mechanism of PEO (homopolymers), according to Chen and co-workers [34]. In PEO/PBE/PVEE blends, intermolecular interactions may be responsible for some degree of confinement on the crystallization of PEO, leading to the results obtained. As a parameter for comparison, in PBE/PEO interpenetrating networks (IPN), the balance between intermolecular interactions involving PBE–PBE and PBE-PEO chains induce structural confinement effects at the nanometer scale, affecting both crystallization and miscibility, as concluded from the paper of Kalogeras and co-workers [35].

Single T_g values were observed for all blends, with a clear dependence on the polymer concentrations, which is an indicative of miscibility. For the binary PBE/PVEE and PEO/PVEE blends, the dependence of T_g with composition was studied by the Fox Equation (3) [36]. T_g-composition dependence for the ternary blends was studied by a linear weight-average model, expressed in Equation (4), used by Goh and Ni [37] and Woo and Wu [38].

$$\frac{1}{T_g} = \sum_i \frac{w_i}{T_{g,i}} \tag{3}$$

$$T_g = \sum_i w_i T_{g,i} \tag{4}$$

In Equations (3) and (4), w_i and $T_{g,i}$ are the weight fraction and the T_g of the component *i*, respectively. The calculated T_g values are listed in Table 1, based on the T_g values of pure polymers PEO, PBE and PVEE, which are −45, 33 and −49 °C, respectively.

PEO/PVEE blends can be considered miscible, due to the presence of a single T_g for the compositions studied in the present work, as mentioned. Due to the close T_g values of PEO and PVEE, the dependence of this parameter on the composition in their binary blends can not be easily evaluated, however, there is a god agreement between the experimental and predicted (by the Fox equation) values, except for the system containing 40 wt% PVEE, which exhibits $T_g = -42$ °C. The ΔT_g values for these blends are smaller than those detected for the pure polymers, which indicates that the non-crystalline (glassy) fraction is highly homogeneous and corroborates the hypothesis of miscibility. The melting temperature exhibits a decrease as the PVEE concentration increases in the blend, from 72 °C (PEO) to 61 °C (40 wt% PVEE), suggesting the formation of smaller or imperfect crystalline structures due to the presence of PVEE. The decrease in T_m is followed by a decrease in ΔH_m values, from which the crystallinity degrees of the blend ($X_{c,blend}$) and of the PEO fraction in the blend ($X_{c,PEO}$) were calculated. In PEO/PVEE blends, the crystallinity decrease observed from 72% (PEO) to 49% (40 wt% PVEE) is clearly a consequence of a dilution effect, since the $X_{c,PEO}$ values follow an inverse tendency, increasing up to 84% (30 wt % PVEE) and 82% (40 wt% PVEE). Combining the trends in $X_{c,blend}$ and $X_{c,PEO}$ values, considering also the miscibility of the system, one can conclude that PVEE chains form a miscible phase with PEO, which preferentially occupies the non-crystalline regions of the solid, inhibiting the crystal growth of PEO chains. In order to evaluate the crystalline formations in PEO/PVEE binary blends, optical micrographs are presented for this system in Supplementary material, Fig. S4. PLOM images evidence the formation of a partially crystalline structure, due to the presence of the characteristic Maltese cross patterns, which are clearly affected by the addition of PVEE. Addition of PVEE from 5 to 40 wt% to PEO strongly inhibit the formation of larger crystalline structures, as those seen in pure PEO micrograph, indicating that the crystal growth step is affected by the presence of an increasing PVEE concentration in the blend [39]. This behavior is coherent with the DSC measurements interpretation, which pointed to the formation of smaller or imperfect crystalline structures as the PVEE concentration increases in the PEO/PVEE blend, compared to pure PEO. For the sample containing 40 wt% PVEE, this behavior is more evident, as the formation of a larger number of crystal centers with smaller diameter than those observed for pure PEO is detected. From the PLOM images interpretation, based on the DSC discussion, a miscible PEO/PVEE non-crystalline phase is detected, in which PEO crystalline centers, smaller than those observed in pure PEO, are dispersed.

From the data listed in Table 1, the measured and calculated T_g values for PBE/PVEE blends can be compared and small differences are observed between the calculated and experimental values. For the PBE/PVEE blend containing 5 wt% PVEE, the experimental T_g exhibits a negative deviation of about 10 °C from that calculated by the Fox model. For the blends containing 10 and 15 wt% PVEE, however, the deviation observed is positive. Both deviations (positive and negative) suggest strong interactions between the blend components, since the Fox model describes the T_g behavior for ideal mixtures, where no effective interactions take place [40]. For the binary PBE/PVEE blends, ΔT_g values are in the range between 23.6 and 29.2 °C. If these ΔT_g values are taken into account on the comparison between calculated and experimental T_g values, a good agreement is found for this system. It is not expected that a T_g *vs* composition plot would exhibit a linear dependence for ternary blends, however, the linearity suggested by Equation (4) was used as a standard to measure the deviation between the calculated and experimental T_g values [37,38]. A very interesting T_g behavior was observed for the ternary PEO/PBE/PVEE blends, for which these values present only a small dependence on the blend composition, not greater than the experimental error of the measurement. Even for 40 wt% on total non-crystalline polymers (PBE or PVEE) added to the blend, the T_g remains between −42 and −44 °C. Some of the calculated T_g values for the ternary blends present a good agreement with the experimental ones, especially if ΔT_g is taken into account in the comparison. This stands for blends with PEO/PBE/PVEE compositions 90/5/5, 80/10/10 and 70/15/15.

There are three factors which determine the miscibility of a ternary polymer blend:

(i) at least two of the three pair wise interaction parameters (χ_{12}, χ_{13} and χ_{23}) must be smaller than χ_{crit} (Equation (5), where N_i is the degree of polymerization), *i.e.*, two of three of the polymer pairs must be miscible and the last one should be only marginally immiscible, in order to obtain a miscible ternary mixture;
(ii) the component ratios and
(iii) the molecular weight of the polymers (which also influence on the miscibility of the ternary blend [41]).

$$\chi_{crit} = \frac{1}{2}\left(N_1^{1/2} + N_2^{1/2}\right) \tag{5}$$

The symmetry of the interaction parameters ($\Delta\chi = |\chi_{12} - \chi_{13}|$) between the two miscible binary pairs can provide a guide to miscibility. If there is any asymmetry in the interaction parameters ($\chi_{12} \neq \chi_{13}$), the so-called "$\Delta\chi$" effect promotes a phase separation. Even if each of the binary pairs is miscible, in combination they may produce an immiscible ternary blend provided that the value of $\Delta\chi$ is sufficiently large [42]. In the PEO/PBE/PVEE blend, there may be a $\Delta\chi$ effect for higher PBE or PVEE concentrations, since the values of χ for the binary miscible PBE blends are $\chi_{PEO/PBE} = -1.90$ and

$\chi_{PBE/PVEE} = -1.74$ [23,37]. The main goal of the present work is the study of PEO-rich ternary blends, due to the possible application of this system as host matrices in solid electrolytes. Miscibility is an important characteristic of a polymer blend for application as host in electrolytes, and can also be affected by the presence of a metal salt dissolved in the solid [43]. In PEO/PBE/PVEE blends with PEO concentrations of 60 wt% or more, only one glass transition was found, which is a strong indicative of miscibility among the components.

ΔC_p is associated with the changes of degree of freedom in the glass transition resulting from the free volume changes in this temperature. For the PBE/PVEE binary blends, ΔC_p is greater than that of the pure polymers (Table 1), which represent a non-linear dependence with the blend composition, including low PVEE concentrations. The composition dependence of ΔC_p is expected to be linear if no strong interactions take place, *e.g.*, in ideal binary blends, for which volume additivity is also expected and, in this case, ΔC_p would reflect only changes of the conformational arrangement and, consequently, in the system entropy. The dependence of ΔC_p on the blend composition, listed in Table 1, clearly reflects the non-additivity of volume, which indicates intermolecular interactions between PBE and PVEE. For the ternary PEO/PBE/PVEE blends, ΔC_p is lower than the value observed for the pure polymers, which indicates that the non-crystalline phase is structurally similar to the viscoelastic phase, since the free volume changes in the glass transition are smaller than that observed for the pure polymers [44].

Fig. 1 shows the phase diagrams of the ternary blends containing (a) 60 wt% PEO, and (b) equal contents of PBE and PVEE. In both diagrams, the glassy, viscoelastic and melt regions are well defined. Above the T_m line the system is a miscible liquid phase; below T_g line, is a vitreous phase and between T_m and T_g lines, there is one viscoelastic phase. A large temperature extent of the viscoelastic phase is a requirement for the application of the polymeric matrix as a host for solid electrolytes. In the ternary blends containing 60 wt% PEO (Fig. 1 (a)), the temperature extent of the viscoelastic phase is increased with the addition of PVEE, since the T_g values of the ternary blends are lower than that of the binary 60/40 (PEO/PBE) blend [21], strongly influenced by the T_g of PVEE. From Fig. 1 (b) it can be seen that the addition of both PBE and PVEE induces no suitable variation in the temperature extent of the viscoelastic phase, but represents a decrease of more than 50% in the crystallinity of the system. As observed by Kuo and co-workers [45] for ternary blends of PBE, poly(vinyl acetate) (PVAc) and poly(vinyl pyrrolidone) (PVP), the presence of PBE tends to increase the miscibility of the pair PVAc/PVP shifting the miscibility window to the PVP-rich region of the phase diagram, mainly due to $\Delta\chi$ and ΔK effects. In the present work, PVEE is added to the miscible PEO/PBE blend in order to obtain a ternary miscible blend with higher chain mobility and extent of the viscoelastic phase for application as host in solid electrolytes. The DSC analysis thus indicates achievement of these two major characteristics.

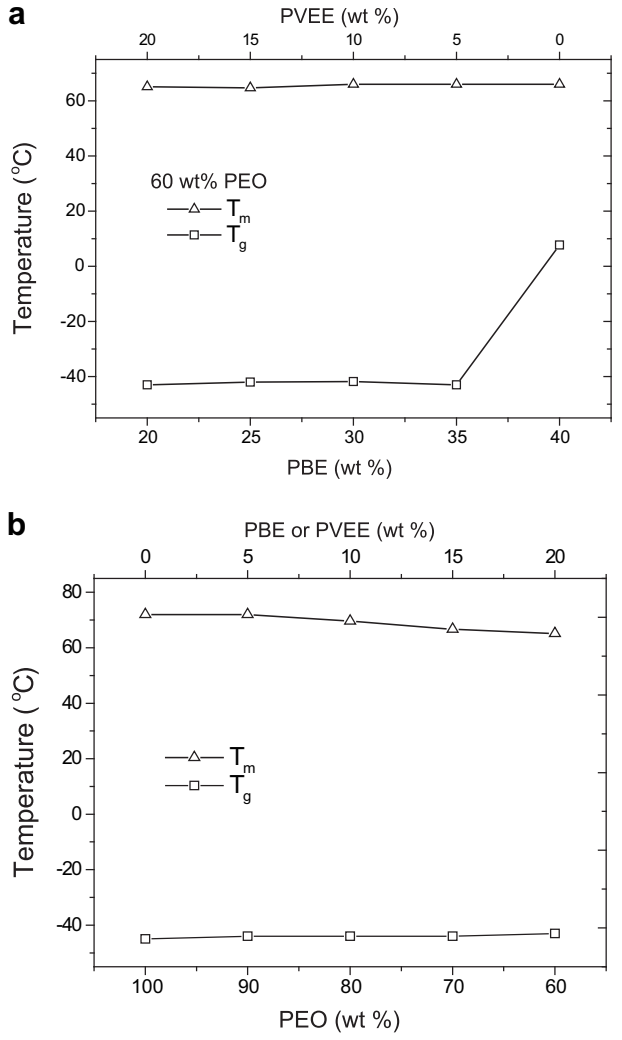

Fig. 1. (a). Dependence of T_m and T_g with PBE and PVEE concentration for PEO/PBE/PVEE blends containing 60% wt in PEO. (b). Dependence of T_m and T_g with the system's composition for PEO/PBE/PVEE blends containing equal amounts of PBE and PVEE.

3.1.2. *Vibrational analysis*

Hydrogen bonding between PBE and PEO was determined to be the intermolecular interaction that takes place in the binary

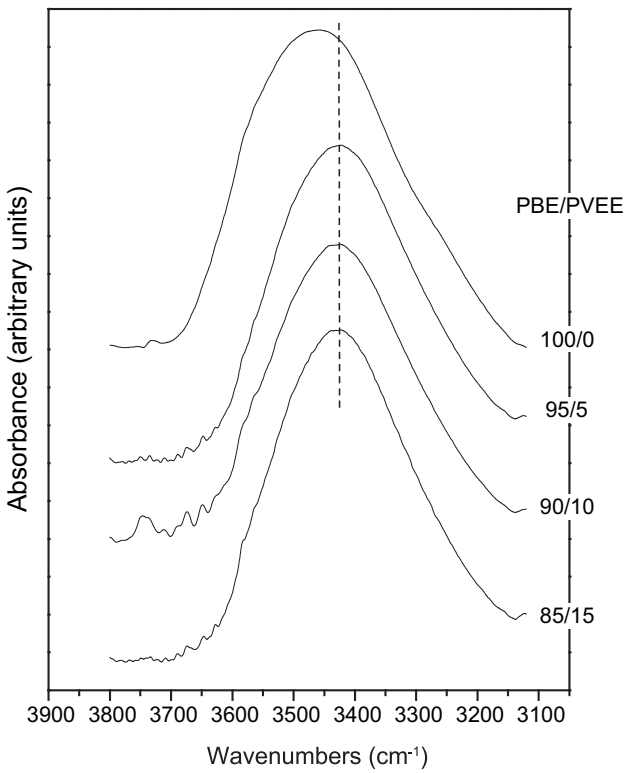

Fig. 2. FTIR spectra of PBE/PVEE blends in the region of 3900–3100 cm^{-1} ν(OH).

PEO/PBE blends and is responsible for the miscibility of the system, as well as the decrease in the crystallinity of the system, as shown previously [21]. In ternary PEO/PBE/PVEE blends, FTIR is used to describe the spectroscopic behavior of the system, aiming to elucidate the specific interactions among the polymers.

In order to characterize the interactions between the polymers in the ternary blend, it is important to describe the behavior of the binary pairs to attain a wider understanding about the system. As mentioned, the PEO/PBE blend was previously studied and, in the present work, results on the PBE/PVEE blend are reported, as a part of the ternary system characterization.

FTIR spectra of PBE/PVEE blends in the OH stretching region (3800–3100 cm^{-1}) is shown in Fig. 2. There are two main contributions on the OH stretching spectra, associated with spectroscopically "free" (not interacting *via* hydrogen bonding) and "bound" (interacting *via* hydrogen bonding) hydroxyl groups. Additionally, the maximum of this band presents a shift from 3475 cm^{-1} (pure PBE) to 3425 cm^{-1} (blend containing 15% wt PVEE), indicating the formation of hydrogen bond interactions involving the hydroxyl group of PBE (as acid) and the ether group of PVEE (as base). A similar interacting system, formed by PEO and poly(hydroxyether sulfone) (PHES), was studied by Lu and co-workers [46], in which specific hydrogen bond interactions were found between hydroxyl groups in PHES self-association (–OH…–OH), as well as hydroxyl–sulfonyl interactions. In their work, the free hydroxyl groups were associated with the vibrational band centered at 3570 cm^{-1}, and a wavenumber shift ($\Delta\nu$) of 221 cm^{-1} (to 3349 cm^{-1}) was attributed to the –OH…–OH interaction. The shoulder at 3487 cm^{-1} ($\Delta\nu = 83$ cm^{-1}) was assigned by the authors as the interaction between hydroxyl and sulfonyl groups. In the present work, the quantitative evaluation of the spectroscopic forms of hydroxyl groups was carried out by decomposing the band into two Gauss functions, in order to separate the free and bound spectroscopic contributions. The variation of spectroscopically free and bound forms of hydroxyl groups with the amount of PVEE in the PBE/PVEE blend is exhibited in Fig. 3.

The spectroscopically bound form of hydroxyl group in pure PBE can be associated with the sum of vibrational contributions of local structures represented by: (i) PBE(OH)…(COC)PBE; (ii) and PBE (OH)…(OH)PBE, which were described as the spectroscopic forms present on the ν(OH) spectral region in pure PBE [21]. In PBE/PVEE blends, another spectroscopic contribution can be represented by the structure (iii) PBE(OH)…(COC)PVEE. As the ratio of PVEE increases in the blend, the bound form of OH group increases, which is associated with an increase on the concentration of structure (iii). Different from PEO/poly(4-vinylphenol-*co*-2-hydroxyethyl methacrylate) blends [47], in which there is a change in the preferential hydrogen binding site with PEO concentration, the hydrogen bonds formed in PBE/PVEE blend (as the PVEE concentration increases) is a result of the interaction between the free OH groups in PBE and the ether groups in PVEE, and not a competition among the binding sites on PBE (COC and OH) with the one on PVEE (COC). The structure represented as (iii) is confirmed by the spectroscopic fractions and also by the miscibility and T_g-composition behavior. In Fig. 4, the equilibrium among the interacting structures in PBE/PVEE blends is represented. Combining the DSC and FTIR data, it is found that structure (iii) is progressively increasing with the concentration of PVEE on the blend, as the free hydroxyl form decreases and the equilibrium involving structures (i) and (ii) are not strongly affected by PVEE in concentrations up to 20 wt%.

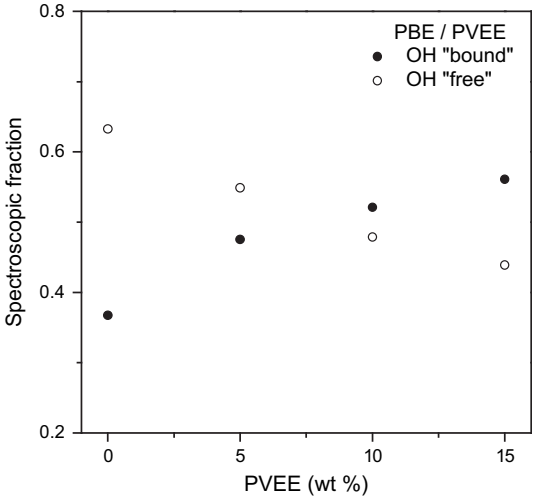

Fig. 3. Spectroscopic fractions of "free" and "bound" hydroxyl groups in binary PBE/PVEE blends.

Based on the knowledge of the intermolecular interactions between PBE and PVEE, it is possible to suggest that, in the ternary system, PEO and PVEE will compete for the interaction sites (–OH) on the PBE chains, affecting the equilibrium described for the PBE/PVEE blend. Since the interactions in the ternary blend can not be easily determined and, due to the complexity of the system, the PEO/PBE and PBE/PVEE descriptions are used in the present work to allow an adequate characterization of the intermolecular interactions among PEO, PBE and PVEE in the ternary blends.

FTIR spectra of the PEO/PBE/PVEE blends are represented in Supplementary material, Fig. S5. The FTIR spectra of the blends in the region between 1400 and 1300 cm^{-1} (Supplementary material, Fig. S6) show the presence of two contributions centered 1359 and 1343 cm^{-1}, associated to the CH_2 wagging mode of PEO [48]. The presence of these bands at 1359 and 1343 cm^{-1} indicates that part of the PEO chains exhibit a helical 7/2 conformation, which is present in its crystalline phase. Despite the presence of these spectroscopic contributions indicate the partial crystallinity of PEO chains, a change in the relative intensity is observed, accompanied by a slight broadening, as the blend composition varies. This behavior corroborates with the other spectroscopic and thermal observations which indicate the crystallinity decrease of the samples with the increase in PBE and/or PVEE concentration. In complete non-crystalline PEO samples, these two bands should merge into a broad contribution centered at approximately 1349 cm^{-1}, reflecting the absence of preferential chain conformation, as pointed out by other authors [49]. As other localized vibrational modes, the $\nu(CH_2)$ may present variations depending on the chain conformation [6] and the nanostructure of the solid [50].

In Fig. 5, the vibrational spectra from 1250 to 900 cm^{-1} of ternary PEO/PBE/PVEE blends and the pure polymers are shown. Acrystalline PEO phase is confirmed by the presence of the triplet peak of the COC stretching vibration at 1148, 1110, and 1062 cm^{-1} with a maximum at 1110 cm^{-1} [6,50]. Changes in the intensity, shape, and position of the COC stretching mode can be associated with the interaction between PEO and PBE. Addition of both PBE and PVEE induces a shift in the central peak of this band, without a clear tendency with the polymers concentration. A broadening is also observed in this band, indicating the participation of the ether group of PEO in intermolecular hydrogen bond interactions. The broadening of this band also reflects the decrease in the crystallinity of the sample [51], which is in agreement with the DSC measurements.

In order to elucidate the hydrogen bond interactions among PEO, PBE and PVEE, the FTIR spectra of the ternary blends in the OH stretching region (3900–3000 cm^{-1}) were studied and are shown in Fig. 6. In these spectra, the number of spectroscopic contributions presents a dependence on the blend composition. Hydroxyl

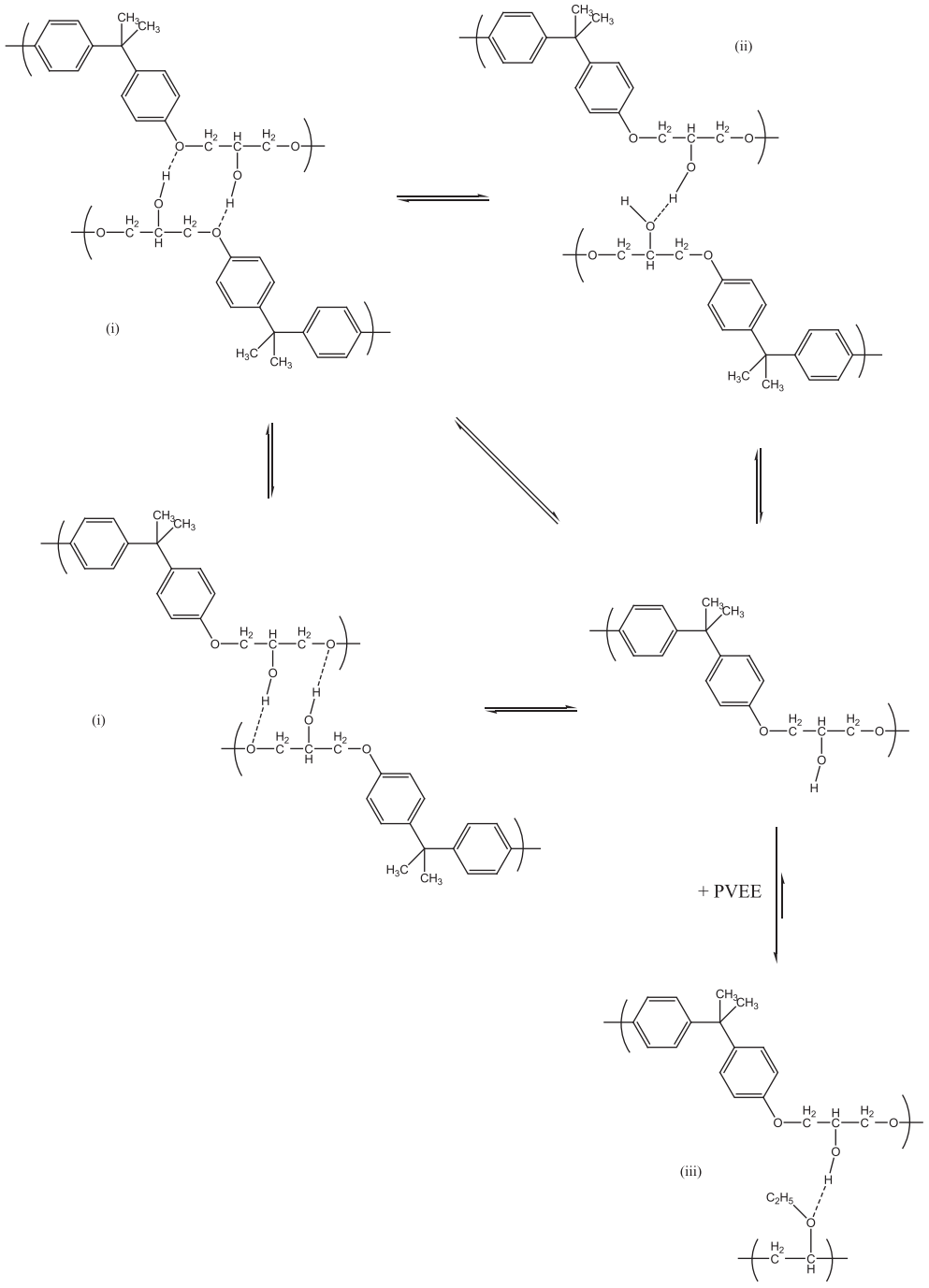

Fig. 4. Molecular model for the hydrogen bond interactions between PBE and PVEE in equilibrium.

stretching band of pure PBE presents two spectroscopic contributions, from free and bound OH forms. All the ternary blends, except 90/5/5, present, with one central peak and two spectroscopic contributions of lower intensity, one at higher wavenumbers and other at lower. These contributions can be associated with the different molecular structures resulting from the intermolecular interactions *via* hydrogen bonding among the polymers. These structures can be described as:

(i) PBE(OH)…(COC)PBE;
(ii) PBE(OH)…(OH)PBE;
(iii) PBE(OH)…(COC)PVEE and
(iv) PBE(OH)…(COC)PEO,

And can be considered the molecular basis for the miscibility of the system, where PBE interacts with both PEO and PVEE, inducing a transient crosslinking *via* hydrogen bonds. The wavenumber shifts ($\Delta\nu$) between the free and the hydrogen bonded hydroxyl stretching vibration can be interpreted as an average measure of the intra- and/or intermolecular strength interactions [52,53]. Each equivalent spectroscopic contribution presents a characteristic $\Delta\nu$ as seen in Fig. 6, associated with the mentioned interacting structures. The number of different interactions between polymers is determined by the stoichiometry and by the balance of thermodynamic energy terms in the blend, namely enthalpy, combinatorial and non-combinatorial entropy, which in turn are related to the energy of the various interactions and to the

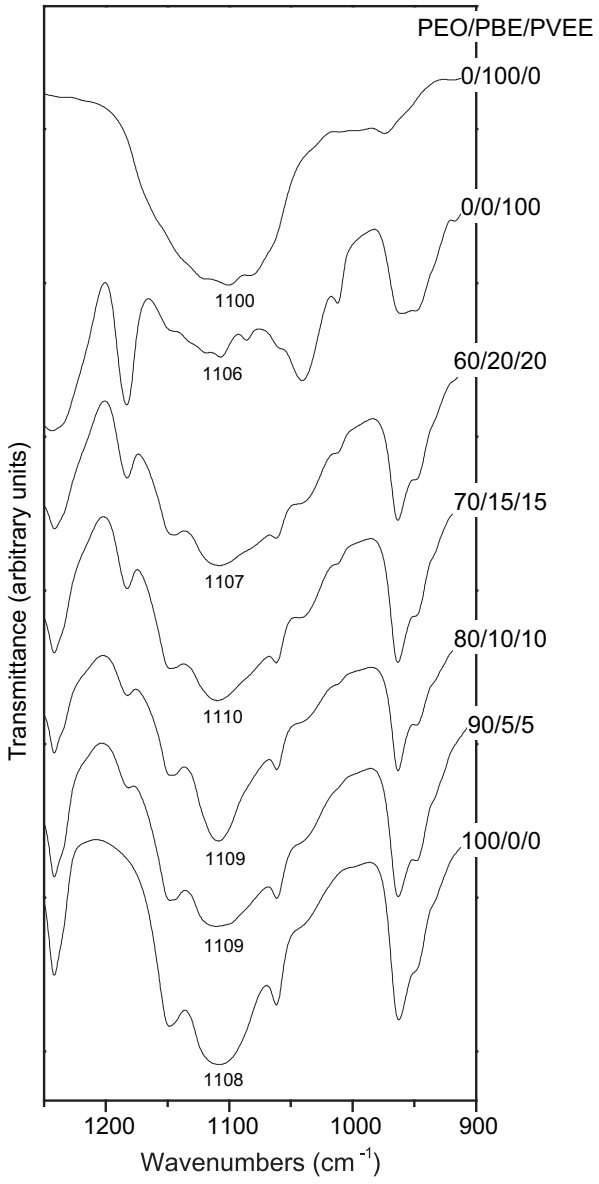

Fig. 5. FTIR spectra of PEO/PBE/PVEE blends in the region of 1250–900 cm^{-1} ν(COC).

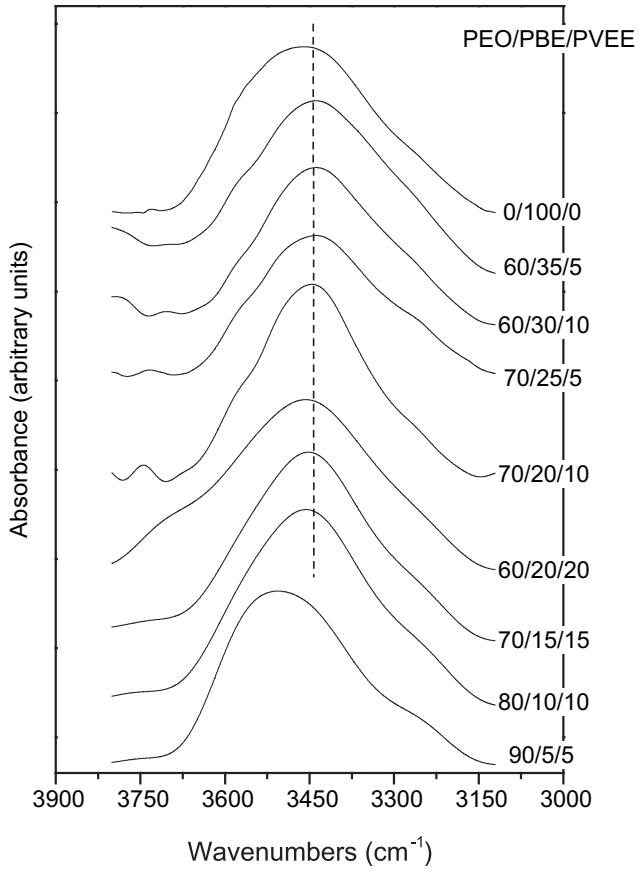

Fig. 6. FTIR spectra of PEO/PBE/PVEE blends in region of 3900–3000 cm^{-1} ν(OH).

backbone and steric hindrance [54]. Due to the number of spectroscopic contributions observed in the hydroxyl stretching band, originated by free −OH, −OH…OCC and −OH…OH interactions, these can be interpreted as groups of structures in equilibrium. Since −OH…OCC interactions are energetically equivalent (as observed by the $\Delta\nu$ values), PBE/PVEE and PBE/PEO interactions are probably randomly distributed along the solid, consisting the molecular basis for the miscibility of the ternary blend, as detected by thermal analysis.

3.2. Polymer electrolytes

3.2.1. Thermal analysis

Among the compositions studied, the 60/25/15 (PEO/PBE/PVEE) ternary blend exhibited a low crystallinity degree, as evidenced by both $X_{c,blend}$ and $X_{c,PEO}$ values. The utilization of 15 wt% PVEE (in mass of the polymers) in the system aims to obtain a partial plasticizer effect in the matrix. From the considerations about chain rigidity, low crystallinity PEO-based blends are usually pointed as the most promising systems to be used as host in solid electrolytes. In the present work, in addition to the low crystallinity observed for the 60/25/15 blend, a synergic effect is intended, combining the contributions of PBE and PVEE, which act increasing the chain mobility, promoting the miscibility and also coordinating lithium ions, with specific cation-binding sites (ether and hydroxyl oxygen atoms).

An endothermic peak, associated with the melting of the PEO crystalline phase is observed in the DSC curves of electrolytes containing up to 10 wt% $LiClO_4$ (Supplementary material, Fig. S7). The apparent melting enthalpy and temperature for each sample were determined from the area and the maximum of these peaks, respectively. A slight decrease in the area of the melting peak is detected with the salt increase, which is associated with the decrease of the melting enthalpy and, consequently, the crystallinity of the system. The melting temperatures (T_m) of each electrolyte also present variations depending on the salt concentration. The crystallinity behavior of the present system is similar to the electrolytes based on the binary PEO/PBE blend [27], where a decrease in the overall crystallinity is detected with the increase of salt content. This decrease in the electrolytes crystallinity with the salt content can be attributed to the coordination of cations by basic sites of the polymers in the matrix, which restricts certain chain segment translations and inhibit the crystallization [55]. Coherent with this hypothesis, recrystallization peaks are found for electrolyte samples containing 5 and 10 wt% $LiClO_4$. The presence of these exothermic peaks in the heating curves indicates that PEO present in the electrolyte samples exhibits difficulty to crystallize during the cooling scan and corroborates with the hypothesis of cation coordination by the polymers in the matrix.

Table 2 lists the T_g, ΔT_g, ΔC_p, T_m, ΔH_m, X_c and $X_{c,PEO}$ values for the electrolyte samples.

Electrolytes exhibited a multiphase behavior, dependent on the lithium perchlorate concentration. Samples containing up to 10 wt % $LiClO_4$ presented a single glass transition temperature, indicating that the salt addition (up to 10 wt%) to the blend does not induce phase separation. The increase in salt concentration in these miscible electrolytes, despite not causing phase separation, interferes in chain mobility, as detected by the increase in $T_{g,1}$ from −42 °C (ternary blend) to −31 °C (10 wt% $LiClO_4$). Additionally, for these miscible samples, $\Delta T_{g,1}$ is observed to increase from 9 to 35 °C, suggesting the existence of a progressively larger number of chain arrangements in the miscible phase, also coherent with the increase in $\Delta C_{p,1}$. While T_m values for these miscible compositions do not exhibit a considerable variation (ranging between 68 and 62 °C), the melting enthalpy (ΔH_m) decreases from 61.5 to 34.5 J g^{-1}, reflecting crystallinity degrees of 33 and 18%, respectively. The crystallinity decrease in miscible polymer electrolytes has been extensively reported [56] and is usually attributed to the formation of polymer-cation coordinated (Lewis) structures with lower structural order at long range, which induces lower crystallinity. The crystallinity associated with the PEO fraction present in the electrolytes ($X_{c,PEO}$) also undergoes a decrease, from 50% (ternary blend) to 28% (10 wt% $LiClO_4$), indicating an actual crystallinity decrease and not merely a dilution effect. The miscibility and crystallinity behavior in these miscible (one-phase) electrolytes can be interpreted by means of a molecular interaction model in which lithium cations act as a "transient crosslinking" agent among the polymer chains, inducing the increase in T_g, ΔT_g and ΔC_p. One example of increasing T_g with salt concentration is found for the solid electrolyte based on a polymeric blend PEO/PPO/PMMA/$LiClO_4$, studied by Wieczorek and Stevens [11], in which Li^+ acts as transient crosslinking centers, decreasing chain mobility. Electrolytes containing from 15 to 30 wt% $LiClO_4$ exhibited more than one glass transition, associated with PEO-rich ($T_{g,1}$) and PBE-rich ($T_{g,3}$) phases. The PBE-rich phase behaves almost independently, exhibiting T_g and ΔT_g increase with the salt concentration. The phase associated with $T_{g,2}$ presents a more complex behavior, probably due to composition fluctuations between PEO-rich and PBE-rich phases. Other electrolytes have presented similar behavior, passing from a miscible system at lower salt concentrations to an immiscible one at higher salt contents [29]. This behavior can be associated with the preferential formation of a PEO/Li^+/PEO phase at higher salt concentrations, with consequent phase separation of one or two of the polymer components.

3.2.2. PLOM

Fig. 7 depicts the Polarized Light Optical Microscopy (PLOM) of the electrolyte samples and a pure PEO film obtained under similar conditions. The crystallization pattern of PEO is clearly seen, marked by the Maltese cross-extinction pattern and a fine spherulitic texture. The ternary blend, which contains 60 wt% PEO, also exhibits the typical spherulite formation for the crystalline PEO phase, however distorted due to the presence of PBE and PVEE. The interaction between PEO and these non-crystalline polymers partially inhibits the formation of a crystalline phase, leading to an overall crystallinity decrease (as noted in Table 1), which is mainly a consequence of two structural factors: (i) the formation of smaller crystalline domains and (ii) the formation of defective PEO spherulites. The crystallinity decrease can be inferred mostly from the irregularities present on the crystalline phase formation than from the extension of such phases. The addition of non-crystalline polymers to PEO, forming blends in which intermolecular interactions take place, usually induces a crystallinity decrease, also due to changes in the crystallization mechanism from pure PEO to its blends [13,39].

Irregular spherulites can be clearly seen in the optical micrograph of electrolyte samples containing 5 wt% $LiClO_4$, despite the coarseness and lack of boundary definition between the crystalline domains, while samples containing 10 wt% $LiClO_4$ exhibit small, highly dispersed spherulitic formations through the film. Increasing the salt concentration in the electrolytes induces the formation of less regular structures, due to a coarseness of crystalline lamellae [57]. The morphological changes observed by optical microscopy corroborate with the DSC results, which showed a crystallinity decrease as a function of salt concentration. The increase in the number of spherulites per area, observed more clearly for the sample containing 10 wt% $LiClO_4$, is a direct consequence of an increase in the kinetics of the nucleation step, which reflects in a greater number of nucleation centers formed but smaller spherulites [58]. As in other polymer electrolytes, the lithium cations act as transient crosslink points among the polymer chains, reducing their mobility, which results in smaller spherulites due to reduced chain diffusion during crystallization. The progressive increase in salt concentration leads to evident morphological changes, especially for samples containing salt concentrations higher than 10 wt%, in which no crystalline formation can be detected with the current magnification. For a high $LiClO_4$ concentration (30 wt%), however, a phase separation is clearly seen, induced by the formation of a PEO-rich, salt-containing phase, as detected by the DSC measurements.

3.2.3. FTIR

The ν(COC) vibrational mode of PEO is highly sensitive to the polymer chain conformation, which, by its turn, is dependent on both crystallinity and local arrangements [6]. The local structure of PEO, as reported in the literature [59], is markedly affected by cation coordination, which is able to change the electron density at the ether oxygen atoms and, consequently, the carbon-oxygen bonds and vibrations. The FTIR spectra in the region between 1300 and 900 cm^{-1}, depicted in Fig. 8, clearly show the effect of increasing salt concentration in the electrolytes on the ν(COC)

Table 2
Thermal properties of the PEO/PBE/PVEE/$LiClO_4$ samples.

$LiClO_4$ (wt%)	$T_{g,1}$[a] (°C)	$\Delta T_{g,1}$[a] (°C)	$\Delta C_{p,1}$ ($\times 10^{-2}$ J g^{-1} °C^{-1})	$T_{g,2}$[a] (°C)	$\Delta T_{g,2}$[a] (°C)	$\Delta C_{p,2}$ ($\times 10^{-2}$ J g^{-1} °C^{-1})	$T_{g,3}$[a] (°C)	$\Delta T_{g,3}$[a] (°C)	$\Delta C_{p,3}$ ($\times 10^{-2}$ J g^{-1} °C^{-1})	T_m[a] (°C)	ΔH_m (J g^{-1})	X_c (%)	$X_{c,PEO}$ (%)
0	−42	9	1.3	–	–	–	–	–	–	65	61.5	33	50
5	−35	25	2.3	–	–	–	–	–	–	68	53.5	28	43
10	−31	35	9.5	–	–	–	–	–	–	62	34.5	18	28
15	−41	16	1.5	16	26	7.5	38	5	1.1	–	–	–	–
20	−43	20	9.6	–	–	–	35	8	1.4	–	–	–	–
25	−46	16	1.3	−6	30	7.7	42	7	1.3	–	–	–	–
30	−35	12	1.7	43	15	2.6	45	9	1.0	–	–	–	–

[a] Temperature precision of ±1 °C.

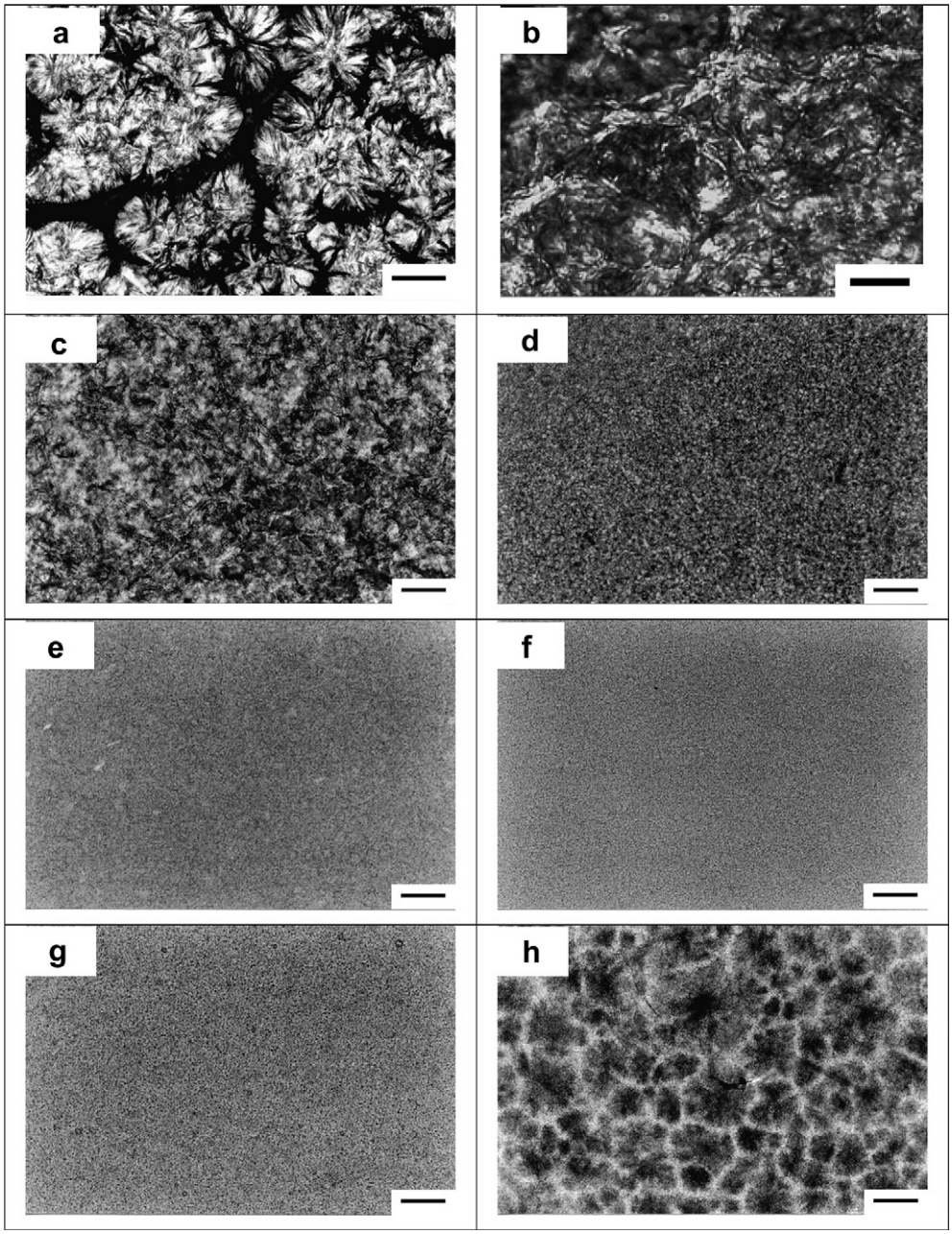

Fig. 7. Polarized light optical microscopy (PLOM) of PEO (a), the ternary PEO/PBE/PVEE 60/25/15 blend (b) and electrolyte samples containing (c) 5, (d) 10, (e) 15, (f) 20, (g) 25 and (h) 30 wt% $LiClO_4$. Scale bars indicate 0.5 mm.

vibrational mode of PEO. Blending PEO with PBE and PVEE leads to broadening of this triplet, as a consequence of crystallinity decrease and specific interactions, as discussed. The salt addition to the blend induces a more pronounced broadening, with overlapped spectroscopic contributions, as seen in the series of spectra in Fig. 8. The observed broadening is proportional to the salt concentration, in which the band linewidth increases from 28 to 83 cm^{-1}, as a result of the increase in the individual spectroscopic contributions from different local arrangements involving the COC and −OH groups and Li^+. As observed by other authors in Ref. [60], lithium cations are preferentially coordinated by ether oxygen atoms from ethylene oxide (EO) chains. In PEO/PBE/PVEE/$LiClO_4$ electrolytes, the changes in ν(COC) vibrational mode as a function of salt concentration evidences the cation coordination by ether oxygen atoms and corroborates the decrease in crystallinity, detected by DSC measurements.

The hydroxyl stretching bands in the FTIR spectra of the ternary PEO/PBE/PVEE (60/25/15) blend and of the solid electrolytes (Supplementary material, Fig. S8), as well as the perchlorate vibrational mode, were studied by mathematical decomposition into Gaussian functions, as described earlier [27]. The ion–polymer interactions can interfere in the polymer–polymer miscibility and, particularly, cations can act as transient crosslink points, enhancing or reducing the miscibility of the system. These interactions are mainly determined by the balance between enthalpic and entropic contributions, associated with local arrangements around the cation, specific polymer–polymer interactions, chain mobility and free volume rearrangement.

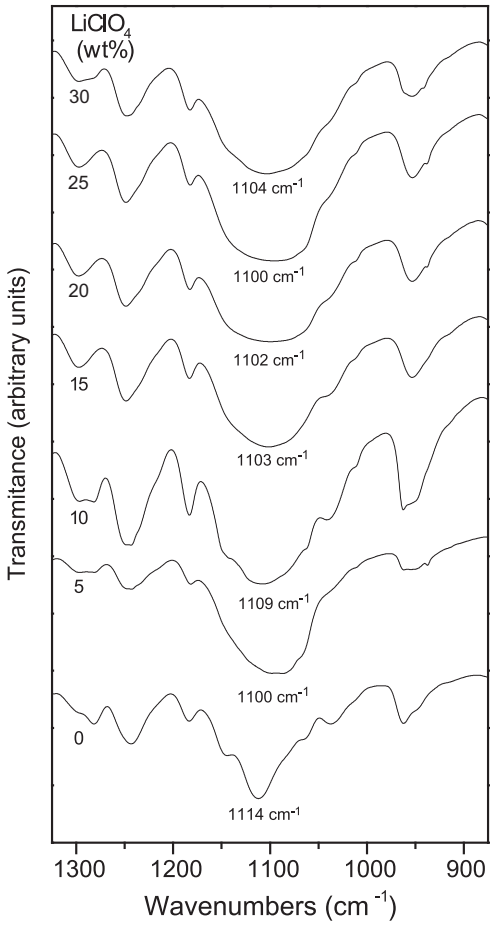

Fig. 8. FTIR spectra of the electrolyte samples in the range of 1300–900 cm^{-1}, evidencing the ν(COC) vibrational mode.

The FTIR spectra of the solid electrolytes in the region between 1400 and 1300 cm^{-1} are represented in Supplementary material, Fig. S9. The CH_2 wagging bands of PEO at 1343 and 1360 cm^{-1}, associated to its crystalline conformation are still present in the FTIR spectrum of the 60/25/15 blend and the electrolytes containing 5 and 10 wt% $LiClO_4$, despite the small changes on the relative intensity and on the shape of these contributions, indicating the presence of some extent of a crystalline PEO conformation and, also, a non-crystalline fraction, as discussed previously. The relative intensity and bandwidth of these contributions are progressively affected by the salt addition and the two bands merge into a single and broader contribution centered at 1351 cm^{-1} for samples containing more than 10 wt% $LiClO_4$. This spectroscopic behavior is another evidence of the crystallinity decrease and subsequent suppression as the salt content increases in the solid electrolytes. As described by other authors in Ref. [61], changes in chain configuration induced by molecular interactions involving PEO (such as cation complexation) markedly affect the CH_2 wagging bands, especially in systems in which the crystallinity decreases, resulting in the observed behavior.

Spectroscopic fractions associated with "free" and "bound" hydroxyl groups were obtained from the ν(OH) spectral region and are represented in Fig. 9. The salt addition drastically changes the equilibrium between free and bound hydroxyl spectroscopic contributions, which is also a consequence of PBE chains distribution among the phases in the solid. In the current approach, for simplicity, hydroxyl groups were simulated considering only spectroscopic contributions involving free groups and those participating in hydrogen bonding. However, in the PEO/PBE/PVEE/$LiClO_4$ electrolyte, there are, additionally, contributions from the interactions: (a) R–O(H)…Li^+; (b) R–OH…ClO_4^- and (c) a combination of the two previous structures, as described for PEO/PBE/$LiClO_4$ solid electrolytes [27]. Despite the polymer–ion interactions, the miscibility among the components can be interpreted by the analysis of the PEO–PBE and PVEE–PBE interactions, which can be conducted by the spectroscopic fractions associated with free and bound –OH groups.

The ternary blend exhibits a bound hydroxyl spectroscopic fraction of about 0.4 and this value increases to 0.83 and 0.79 for the electrolytes containing 5 and 10 wt% $LiClO_4$, respectively. This increase can be associated with the number of PBE–PEO and PBE–PVEE interactions, resulting from the chains approximation imposed by the lithium cation coordination by the ether oxygen atoms of PEO. Additionally, the cation coordination imposes chain movement restriction, which may favor the polymer–polymer interactions in highly homogeneous systems. Since the electrolytes containing up to 10 wt% $LiClO_4$ are miscible and the presence of a single T_g implies homogeneity in the range of 2–15 nm [62,63], the combined effects of motion restriction and homogeneity lead to an increase in the number of hydrogen-bonded hydroxyl groups. In addition, cation coordination by the hydroxyl group would induce a similar effect on the electron density of the oxygen atom, resulting in the intensification of the observed hydroxyl spectroscopic fractions dependence on the salt concentration. Electrolytes containing more than 10 wt% $LiClO_4$ exhibit multiphase behavior, as detected by DSC measurements, which reflects in a more complex spectroscopic behavior, concerning particularly the PBE hydroxyl groups. The progressive decrease observed for the spectroscopically bound hydroxyl group in electrolytes containing $LiClO_4$ between 5 and 25 wt% can be associated with the replacement of –OH…OCC by –OH(free) + CCO…Li^+ interactions, as represented in Fig. 10.

The perchlorate vibrational mode $\nu(ClO_4^-)$ is frequently used to distinguish between associated (ion pairs or aggregates) and dissociated forms of the salt dissolved in solid electrolytes and, from these spectroscopic contributions, mobile ion fractions can be inferred. The FTIR spectra representing the $\nu(ClO_4^-)$ spectroscopic

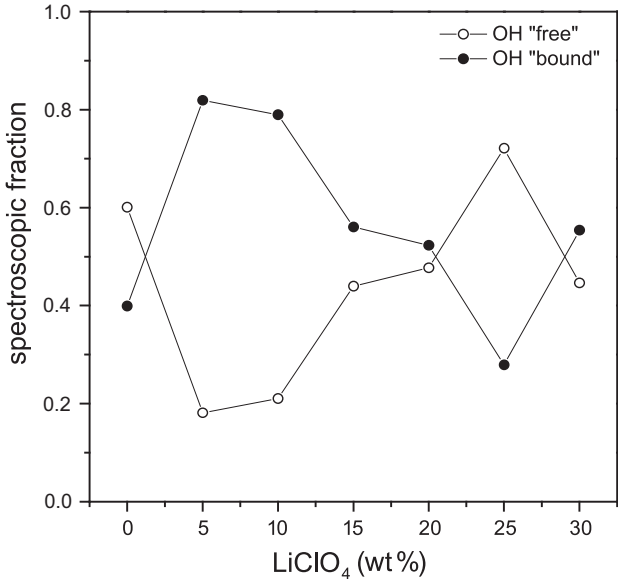

Fig. 9. Spectroscopic fractions of "free" and "bound" hydroxyl groups as a function of salt content.

region are depicted in Supplementary material, Fig. S10. According to Grondin and co-workers [64], dyglyme/$LiClO_4$ samples containing fully dissolved salt exhibit only one spectroscopic contribution of the $\nu_4(ClO_4^-)$ mode at 623 cm^{-1}. In the present work, the band associated to the $\nu(ClO_4^-)$ vibrational mode exhibits contributions at 623 and 634 cm^{-1}, which correspond to dissociated and associated perchlorate anions, respectively. Fig. 11 depicts these spectroscopic fractions dependence on the salt concentration. High salt dissociation (fractions higher than 0.78) is observed for the entire range of concentrations studied, exhibiting only a small decrease as the concentration increases, except the electrolyte containing 15 wt% $LiClO_4$, which exhibits nearly 100% of salt dissociation. This behavior is more likely a consequence of the multiphase structure already discussed, in which a PEO-rich phase containing highly dissolved $LiClO_4$ is formed. While the dissociated spectroscopic fraction represents the ion-separated fraction of salt, the associated spectroscopic fraction can be interpreted as a sum of ion pairs and other aggregates, such as trimmers ($Li_2ClO_4^+$ and $Li(ClO_4)_2^-$) and larger clusters. In general, ionic clusters exhibit lower mobility due to the small charge-to-mass ratio and do not significantly contribute to the overall conductivity of solid electrolytes. In the present system, as can be observed in Fig. 11, the dissolved salt is highly dissociated and, even in large concentrations, up to 30 wt%, there is no evidence of formation of aggregates.

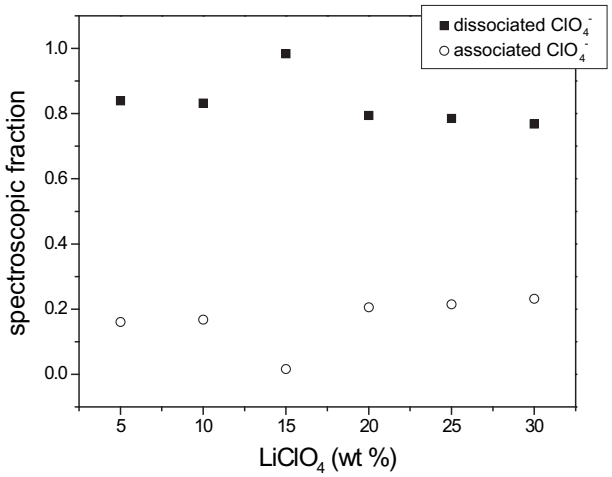

Fig. 11. Spectroscopic fractions of "dissociated" (dissolved) and "associated" (ion pairs or large clusters) perchlorate ions as a function of salt content.

3.2.4. Electrochemical characterizations

Fig. 12 depicts the electrochemical impedance spectra obtained for the electrolytes containing 5, 10 and 20 wt% $LiClO_4$ at room temperature. The impedance spectra exhibit, for all samples, an inclined line in the region of lower frequencies, with constant slopes as a function of temperature. Under the conditions of these experiments, the semicircles represent the resistance of the ion transport in the electrolyte bulk and the inclined lines indicate the resistance against ion passage in the electrolyte/electrode interface. The use of blocking electrodes for the impedance spectra results in a polarization phenomenon in the electrolyte bulk, since there is no ion source or sink. The electrical double layer at each interface possesses infinite resistance against ion transfer, which, in the Nyquist plot of impedance spectra, would result in a straight line, parallel to the ordinate, associated with a limiting capacitance [65].

Ionic conductivity (σ) values were calculated using Eq. (6) from the resistance (R) obtained at the semicircle intercept point in real axis of the impedance spectra and studied as a function of salt concentration and temperature. The Arrhenius model was employed for describing the temperature dependence of σ (Eq. (7)).

$$\sigma = \frac{L}{AR} \tag{6}$$

$$\log(\sigma) = \log(A_0) - \frac{E_a}{RT} \tag{7}$$

Where L and A are the thickness and the (geometrical) area of the sample, respectively; A_0 is a pre-exponential term related to the number of charge carriers in the system; E_a is the apparent activation energy for the conduction process; R is the gas constant and T is the temperature.

The impedance spectra were obtained in temperatures between 25 and 90 °C and the conductivity dependence on the temperature was studied by the Arrhenius model, represented in Fig. 13. As observed, the conductivity values increase as a function of temperature, evidencing the influence of both chain relaxation effect and activation energy for lithium conduction. The Arrhenius model was employed, assuming two conduction regimes: one at lower temperatures and other at higher ones. The only exception is the electrolyte containing 30 wt% $LiClO_4$, which exhibits only one conduction regime at the temperature range studied. The temperatures for which the conduction regime changes are

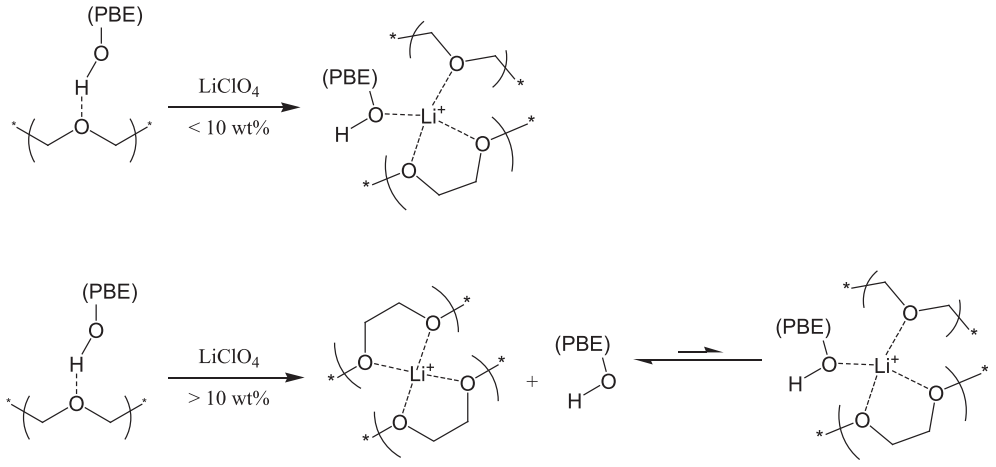

Fig. 10. Schematic representation of the change in specific interactions as a function of the salt concentration.

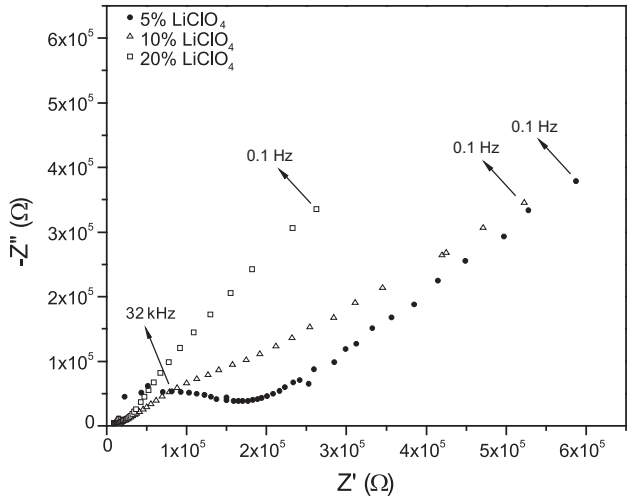

Fig. 12. Electrochemical impedance spectra of samples containing 5, 10 and 20 wt% $LiClO_4$ recorded at room temperature.

coherent with the phase transitions observed for each sample. For the electrolytes exhibiting a crystalline phase, this temperature corresponds, approximately, to the temperature at which the melting of the crystalline phase starts. For the completely non-crystalline electrolytes (with $LiClO_4$ higher than 10 wt%), this temperature is close to the glass transition of each sample. In both cases, the temperature increase reflects on higher chain mobility, with consequent higher conductivities. A similar behavior was described for PEO/$LiClO_4$ electrolytes, which exhibited reproducible conductivity *vs* temperature curves during heating and cooling scans [66], with two conduction regimes, limited by the melting temperature, in highly crystalline and semi-crystalline electrolytes.

Table 3 lists the activation energy (E_a) values and the conductivities at room temperature for the studied electrolytes. The calculated E_a values for the low temperature conduction regimes were found to be higher than the ones for the high temperature regimes. This behavior more likely reflects the chain mobility at higher temperatures, which accounts for the decrease in the energy associated with the ion transport inside the polymer matrix. There are evidences that ion transport in crystalline

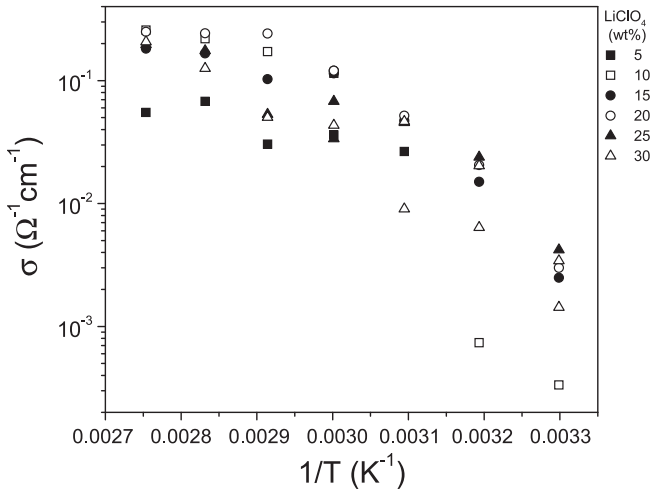

Fig. 13. Dependence of σ with temperature for PEO/PBE/PVEE/$LiClO_4$ samples.

Table 3
Apparent activation energy values (E_a) and ion conductivity (σ) at room temperature for PEO/PBE/PVEE/$LiClO_4$ samples.

$LiClO_4$ (wt %)	E_a (kJ mol^{-1})		σ (Ω^{-1} cm^{-1}) at room temperature
	High temperature	Low temperature	
5	8.87	27.15	3.34×10^{-4}
10	11.72	46.25	2.49×10^{-3}
15	7.44	44.00	3.01×10^{-3}
20	0.72	33.07	4.23×10^{-3}
25	28.38	46.34	3.42×10^{-3}
30	32.27		1.43×10^{-3}

regions does not contribute significantly to the overall conductivity [67] and, since ion transport takes place primarily in non-crystalline phases [68], the temperature increase above melting results in higher conductivity and lower activation energy values. E_a values for the low temperature regime are found between 27.15 and 46.34 kJ mol^{-1} and the increase observed from 5 wt% to electrolytes with higher salt content is more likely a consequence of the ion coordination by the polymers in the blend, which increases chain rigidity, proportional to the number of coordination sites. The E_a values do not increase progressively with the salt concentration, due to the phase separation observed for electrolytes with $LiClO_4$ concentration higher than 10 wt%, but rather reflect the activation energy values of intermediary concentration electrolytes.

Conductivity values at room temperature were found between 10^{-4} and 10^{-3} Ω^{-1} cm^{-1}, exhibiting a progressive increase with salt concentration up to 20 wt%. The maximum σ value at room temperature was obtained for this electrolyte, 4.23×10^{-3} Ω^{-1} cm^{-1}. Since there is no significant change in the spectroscopic fractions of the perchlorate anion, the increase in conductivity is directly related to the increase in the salt concentration and, for instance, the number of charge carriers. For electrolytes containing higher salt amounts, the conductivity decreases, most probably due to a phase separation effect, since the concentration of ion pairs remains almost unchanged with salt content in the electrolyte. The σ values found for the PEO/PBE/PVEE/$LiClO_4$ electrolytes are among the higher described in the literature, even considering other systems with higher mobility, containing ionic liquids and aprotic solvents [69]. This result is mainly due to the high salt solubility in the polymer matrix and to the presence of ion-coordinating sites in the chains of PEO, PBE and PVEE, associated with the partial miscibility of the system and low crystallinity. The obtained conductivity values, in the order of 10^{-3} Ω^{-1} cm^{-1} for electrolytes containing $LiClO_4$ higher than 5 wt%, are reported as sufficiently high for practical applications of the current electrolyte [70]. Comparison between the PEO/PBE/$LiClO_4$ and PEO/PBE/PVEE/$LiClO_4$ electrolytes indicate that the addition of PVEE induces a conductivity increase of approximately 10^2, mainly due to its small chain length, which contributes with a plasticizing effect to the polymer matrix.

The application of solid electrolytes in electrochemical devices is dependent on the thermal and electrochemical properties, among which: conductivity, its dependence on temperature and the electrochemical stability window. This information is accessible through the cyclic voltammogram (CV) of the material (Supplementary material, Fig. S11), in which the current density moduli recorded during the potential scan do not exceed 1.3×10^{-6} A cm^{-2}, even at the higher potential limits imposed to the cell, E ~5.5 V (*vs* Li/Li$^+$). The absence of oxidation or reduction processes in the potential range studied (−0.5–5.5 V *vs* Li/Li$^+$) indicates that the solid electrolyte developed exhibits electrochemical stability wide enough for application is devices such as lithium ion batteries, electrochemical capacitors, artificial muscles, electrochromic devices and others.

4. Conclusions

The PBE/PVEE and PEO/PBE/PVEE blends presented only one glass transition temperature (T_g) and were found to be miscible, as suggested by DSC studies. The T_m values do not present significant changes with the blend composition, however, the degree of crystallinity of the blend decreases from 72% (pure PEO) to 41% (blend 60/35/15), which is coherent with the hypothesis of miscibility. The molecular basis of the miscibility in PEO/PBE/PVEE blends can be associated with the interaction *via* hydrogen bonds among the polymers in the blend, as shown by FTIR analyses. The miscibility and lower crystallinity, compared to pure PEO, as well as the intermolecular interactions in the present system, provide an optimized material for application as host in electrolytes, as evidenced by the characterizations performed on the PEO/PBE/PVEE/$LiClO_4$ system.

From the thermal and spectroscopic characterizations, the lithium ions in the polymer electrolytes were found to play the role of transient crosslink centers, enhancing the miscibility of the system and inducing a more pronounced decrease in the crystallinity. The solid electrolyte obtained with the 60/25/15 ternary blend as host matrix exhibited conductivity values of about $10^{-3}\ \Omega^{-1}\ cm^{-1}$ (20 wt% $LiClO_4$) at room temperature, which are among the highest cited on the literature for polymer/Li^+ electrolyte systems. These systems also exhibited, at 80 °C, conductivity values of about $10^{-1}\ \Omega^{-1}\ cm^{-1}$. This high conductivity was attributed to the low crystallinity of the matrix, which induces high chain mobility, combined to the presence of a large number of Lewis basic sites, especially oxygen atoms.

Acknowledgements

Authors would like to thank CNPq and CNPq/PIBIC for fellowships and FAPERJ for financial support.

Appendix. Supplementary material

Supplementary data related to this article can be found online at doi:10.1016/j.polymer.2010.08.050.

References

[1] Conte FV. Elektrotechnik & Informationstechnik 2006;123:424.
[2] Armand M, Tarascon J-M. Nature 2008;451:652.
[3] Andreev YG. Bruce PG Eletrochim Acta 2000;45:1417. and references therein.
[4] Bruce PG. Solid state electrochemistry. Cambridge: Cambridge University Press; 1997. p. 106.
[5] MacGlashan GS, Andreev YG, Bruce PG. Nature 1999;398:792.
[6] Pereira RP, Rocco AM, Bielschowsky CE. J Phys Chem B 2004;108:12677.
[7] Krishnan M, Balasubramanian S. Phys Rev B 2003;68:064304.
[8] Rocco AM, Pereira RP, Felisberti MI. Polymer 2001;42:5199.
[9] Guo Q, Harrats C, Groeninckx G, Koch MHJ. Polymer 2001;42:4127.
[10] Guo Q, Harrats C, Groeninckx G, Reynaers H, Koch MHJ. Polymer 2001;42:6031.
[11] Wieczorek W, Stevens JR. J Phys Chem B 1998;102:9610.
[12] Triolo A, Visalli G, Triolo R. Solid State Ionics 2000;133:99.
[13] Pereira RP, Rocco AM. Polymer 2005;46:12493.
[14] Rocco AM, Fonseca CNP, Pereira RP. Polymer 2002;43:3601.
[15] Li XJ, Fu WG, Wang YN, Chen TH, Liu XH, Lin H. Polymer 2008;49:2886.
[16] Scott RL. J Chem Phys 1949;17:279.
[17] Tompa H. Trans Faraday Soc 1949;45:1142.
[18] Wu CP, Wu YL, Zhang RY. Macromol Chem Phys 1996;197:3191.
[19] Wu CP, Wu YL, Zhang RY. Eur Polym J 1998;34:1261.
[20] Robeson LM, Hale WF, Merriam CN. Macromolecules 1981;14:1644.
[21] Rocco AM, Moreira DP, Pereira RP. Eur Polym J 2003;39:1925.
[22] Zhang SH, Painter PC, Runt J. Macromolecules 2002;35:9403.
[23] Hong BK, Kim JK, Jo WH, Lee SC. Polymer 1997;38:4373.
[24] Manestrel CL, Bhagwagar DE, Painter PC, Coleman MM, Graf JF. Macromolecules 1992;25:7101.
[25] Jo WH, Kwon YK, Kwon IH. Macromolecules 1991;24:4708.
[26] Lin CL, Chen WC, Kuo SW, Chang FC. Polymer 2006;47:3436.
[27] Rocco AM, Fonseca CP, Loureiro FAM, Pereira RP. Solid State Ionics 2004;166:115.
[28] Cimmino S. Makromol Chem 1990;19:2447.
[29] Wieckzoreck W, Lipka P, Zukowska G, Wycislik H. J Phys Chem B 1998;102:6968.
[30] Munk P. Introduction to macromolecular science. NY: Wiley; 1989.
[31] Pielichowski K, Flejtuch K, Pielichowski J. Polymer 2004;45:1235.
[32] Hsu JY, Nandan B, Chen MC, Chiu FC, Chen HL. Polymer 2005;46:11837.
[33] Zhu L, Cheng SZD, Calhoun BH, Ge Q, Quirka RP, Thomas EL, et al. Polymer 2001;42:5829.
[34] Chen HL, Lin SY, Huang YY, Chiu FC, Liou W, Lin JS. Macromolecules 2002;35:9434.
[35] Kalogeras IM, Stathopoulos A, Vassilikou-Dova A, Brostow W. J Phys Chem B 2007;111:2774.
[36] Fox TG. J Appl Bull Am Phys Soc 1956;1:123.
[37] Goh SH, Ni X. Polymer 1999;40:5733.
[38] Woo EM, Wu MN. Polymer 1996;37:1907.
[39] Cohen LE, Rocco AM. J Therm Anal Cal 2000;59:625.
[40] Hill DJT, Whittaker AK, Wong KW. Macromolecules 1999;32:5285.
[41] Cowie JMG, Li G, Ferguson R, McEwen J. J Polym Sci B Polym Phys 1992;30:1351.
[42] Cowie JMG, Li G, McEwen. Polymer 1994;35:5518.
[43] Subramania A, Sundaram NTK, Kumar GV. J Power Sources 2006;153:177.
[44] Cassu SN, Felisberti MI. Polymer 1997;38:3907.
[45] Kuo SW, Chan SC, Chang FC. Polymer 2002;43:3653.
[46] Lu H, Zheng S, Tian G. Polymer 2004;45:2897.
[47] Rocco AM, Bielschowsky CE, Pereira RP. Polymer 2003;44:361.
[48] Bermudez VD, Carlos LD, Silva MM, Smith MJ. J Chem Phys 2000;112:3293.
[49] Deng Y, Dixon JB, White GN. Colloid Polym Sci 2006;284:347.
[50] Li X, Hsu SL. J Polym Sci Polym Phys Ed 1984;22:1331.
[51] Bailey Jr FE, Koleske JV. Poly(ethylene oxide). New York: Academic Press; 1976. p. 115.
[52] Purcell KF, Drago RS. J Am Chem Soc 1968;24:251.
[53] Coleman MM, Painter PC. Appl Spectrosc Rev 1984;20:225.
[54] Li D, Brisson J. Polymer 1998;39:793.
[55] Vachon C, Labrèche C, Vallée A, Besner S, Dumont M, Prud'homme J. Macromolecules 1995;28:5585.
[56] Wright PV. In: MacCallum JR, Vincent CA, editors. Polymer electrolyte reviews, vol. 2. London: Elsevier; 1989 [Chapter 3].
[57] Choi BK. Solid State Ionics 2004;169:123.
[58] Dreezen G, Fang Z, Groeninckx G. Polymer 1999;40:5907.
[59] Johansson P. Polymer 2001;42:4367.
[60] Munch-Elmér A, Jannasch P. Solid State Ionics 2006;177:573.
[61] Tang J, Lee CKS, Belfiore LA. J Polym Sci Part B Polym Phys 2003;41:2200.
[62] Hsu WP. Thermochim Acta 2007;454:50.
[63] Lewandowska K. Eur Polym J 2005;41:55.
[64] Grondin J, Ducasse L, Bruneel J-L, Servant L, Lassègues J-C. Solid State Ionics 2004;166:441.
[65] Li X, Hsu SL. J Polym Sci Polym Phys Ed 1984;22:1331.
[66] Choi BK, Kim YW. Mater Sci Eng B 2004;107:244.
[67] Yang L, Zhang A, Qiu B. Solid State Ionics 1988;28–30:1029.
[68] Berthier C, Gorecki W, Minier M, Armand MB, Chabagno JM, Rigaud P. Solid State Ionics 1983;11:91.
[69] Reiter J, Vondrák J, Michálek J, Mička Z. Electrochim Acta 2006;52:1398.
[70] Wang YJ, Kim D. J Power Sources 2007;166:202.